Scanning Microscopy

Volume 1990
Number 4 *Fundamental Electron and Ion Beam Interactions with Solids for Microscopy, Microanalysis, and Microlithography*

Article 15

1990

Extracting Chemical Information from Auger Line Shapes

David E. Ramaker
George Washington University

Scanning Microscopy Supplement 4, 1990 (Pages 207-221)
Scanning Microscopy International, Chicago (AMF O'Hare), IL 60666 USA

0892-953X/90$3.00+.00

EXTRACTING CHEMICAL INFORMATION FROM AUGER LINE SHAPES

David E. Ramaker*
Department of Chemistry
George Washington University
Washington, DC 20052
Phone (202) 994-6934

Abstract

We have developed a generally applicable, semi-empirical approach for quantitatively interpreting Auger line shapes. Detailed information on hybridization, electron delocalization and correlation, screening effects, bonding, and covalency can be obtained from the line shape. Methods for extracting the Auger line shape from the experimental data are briefly described. We summarize our recent results from the C KVV Auger line shapes of five different gas phase hydrocarbons (methane, ethane, cyclo-hexane, benzene, and ethylene), three solids (polyethylene, diamond, and graphite), and a molecularly chemisorbed system (ethylene/ Ni). The normal kvv component accounts for only about half of the total experimental KVV intensity for the hydrocarbon gases; much larger fractions for the three solids. The remaining part of the experimental line shape can be attributed to satellites resulting from resonant excitation or dynamic screening processes. The normal kvv component line shapes are seen to reflect delocalized holes, however correlation effects are very evident. Although these screening and correlation effects complicate the interpretation of the line shapes, they indeed cause the chemical effects seen in the experimental line shapes.

Key words: Auger spectroscopy, hydrocarbons, diamond, graphite, carbon, polyethylene, electron screening, electron correlation.

Introduction

Auger electron spectroscopy (AES) has been utilized as a technique for elemental identification and trace analysis at the surface of solids for many years now. Indeed, AES has become a widely available and almost indispensable technique for determining surface cleanliness, surface coverage, and sputter depth profiles. AES has also been recognized as a source of chemical information. Usually this is in the form of spectral "finger prints" to identify the chemical nature of various atoms. This has become so common that many surface chemists can recognize on sight the C KVV dN(E)/dE Auger spectra for graphite, carbides or diamond (Hass et al., 1972), or the Si $L_{23}VV$ Auger spectra for Si, SiO_x, or metal silicides (Bader et al., 1981).

AES has however the potential to provide much more, namely, detailed information on hybridization, electron delocalization and correlation, screening effects, bonding, and covalency. Such information can be obtained from a thorough understanding of the factors contributing to the Auger spectral line shape, and a quantitative interpretation of the line shape. AES has not realized its full potential because these are formidable tasks, but significant progress has been made in recent years.

To obtain chemical or electronic structure information from AES requires two major efforts; first one must extract a true Auger line shape from the raw Auger spectrum, and second, one must derive a theoretical framework for semi-quantitative interpretation of that line shape. We summarize current methods for extracting the line shape and present basic concepts and our theoretical framework for interpreting the line shape. We also review recent applications involving the carbon atom in its varied allotropic and chemical forms. In particular, we examine the C KVV Auger line shapes for several gas phase hydrocarbons (methane, ethane, ethylene, benzene, and cyclohexane) three solids (graphite, diamond, polyethylene), and a chemisorbed system (molecular ethylene on Ni(100). We examine the dramatic effects of final state hole-hole correlation and core-hole screening, how they change from the gas phase molecular, condensed molecular, and solid states, and how these can be used to learn something about the chemical and electronic properties of the material under study.

Extracting the line shape

The difficulty with obtaining a quantitative Auger line shape is well known (Ramaker et al., 1979). It exists because the relatively small Auger signal sits on top of a large background, consisting of the backscattered (redistributed primaries) and secondary electrons arising from the electron beam which initiated the Auger decay. In addition, the Auger signal itself is distorted due to the inelastic losses which the Auger electrons suffer on their way out of the solid.

Removing the background

Several techniques exists for removing the large background. These can be itemized as follows.

Recording the derivative signal The most common technique in practice is to record the derivative, $dN(E)/dE = N'(E)$, spectrum. Since the background is normally slowly varying with energy relative to the Auger signal, N'(E) suppresses the background and emphasizes the Auger signal. Although N'(E) is very useful for spectral "finger printing" as discussed above, a quantitative removal of the background is not accomplished in this way. We have found it more problematical to quantitatively remove the background from N'(E) than from N(E) (Ramaker et al., 1979).

Numerical removal from N(E) The most helpful technique for removal of the background from N(E) is to utilize some analytical expression to approximate the background function, and numerically remove the background by fitting this expression to the upper and lower energy wings of the Auger signal (Ramaker et al, 1979). At energies above 200 eV, often a simple linear background is sufficient. Below 200 eV, the Sickafus (1971, 1977) function, $A*(E+\varphi)^{-n}$ has been found to be a reasonably good approximation to the secondary spectral distribution. We (Ramaker et al., 1979) have previously used a variation of the Sickafus function for the secondaries, and a Bethe function for the redistributed primaries.

X-ray or positron-annihilation induced AES Conventional electron-excited AES not only creates a large background of backscattered and secondary electrons, the intense primary beam can cause damage, charging problems in insulators, and desorption of adsorbed layers. X-ray induced AES (XAES) has become far more popular in recent years, because it utilizes much lower beam fluxes reducing charging, damage, and background signals (Fuggle, 1981). In an exciting new approach, low energy positrons are used to remove core electrons by matter-antimatter annihilation, which then allows the core excitation to relax via the Auger process (Weiss et al., 1988). Positron induced AES (PAES) essentially removes all problems with background removal, since the low energy (< 10 eV) positrons do not produce any secondary electrons above 10 eV.

Coincident techniques The technique of Auger photoelectron coincidence spectroscopy (APECS) utilizes the simultaneous detection of a core photoelectron and an associated Auger electron to eliminate the background. The background is eliminated because only those electrons originating from the same excitation event are counted in the spectrum. Although originally proposed over 10 years ago by Haak et al. (1978), the increasing availability of synchrotron sources makes this technique much more feasible today [R.A. Bartynski and E. Jenson, private communication].

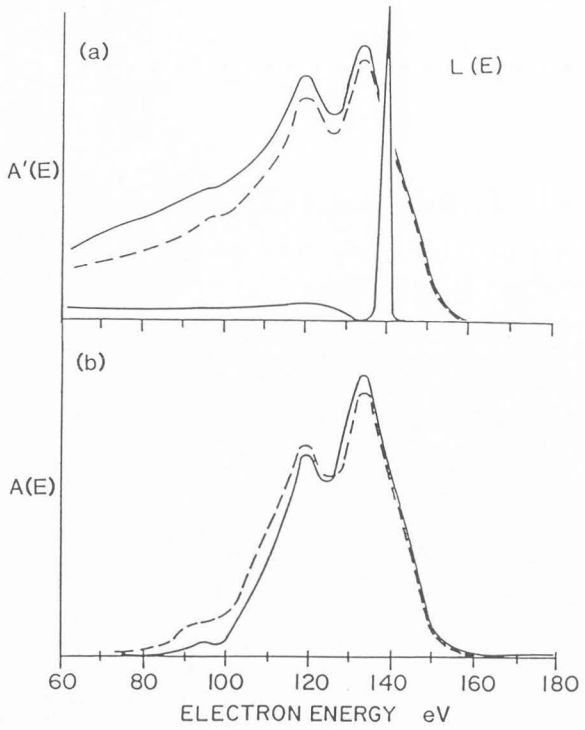

Fig. 1. The S $L_{23}VV$ Auger spectrum from Li_2SO_4 powder pressed onto an In substrate (Ramaker et al., 1979). a) The Auger line shape A'(E) is shown after background subtraction. The elastic peak and loss features, L(E), were observed from a 140 eV primary beam incident on the sample. The latter data were taken with a CMA in the normal mode and are not corrected for the analyzer transmission distortions. b) The "true" Auger signal A(E) obtained after deconvoluting out the electron-loss contributions and correcting for sample and spectrometer transmission. The solid and dashed lines in both a) and b) indicate two different estimates of the background and the resultant final A(E) spectra obtained.

Removal of distortion due to energy loss

Removal of the distortion effects due to electron energy loss of the Auger electrons as they escape from the solid is accomplished (Mularie and Peria, 1970) by deconvolution with a backscattered spectrum, L(E), with primary energy at or near the principal Auger energy as shown in Fig. 1a. Mathematically this can be written

$$A'(E) = \int A(\varepsilon)L(E-\varepsilon)d\varepsilon, \qquad (1)$$

where A' and A are the "experimental" and "true" Auger line shapes. In practice A(E) is obtained by an iterative deconvolution procedure due to Van Cittert (Madden and Houston, 1976). The deconvolution also removes experimental resolution effects of the analyzer since the elastic peak of L(E) has been broadened by this same amount. The relative intensities of the loss and elastic contributions to L(E) must be weighted differently to account for the different geometrical relationships of the Auger and backscattered electrons; i.e. the internally created Auger electrons traverse the solid escape region once, the backscattered electrons twice. In practice this is accomplished (Madden and Houston, 1977) by weighting the loss contributions such that A(E) has zero intensity at the low energy wing of the spectrum as shown in Fig. 1b.

The extraction of the Auger line shape from the experimental data is unfortunately not a straightforward and simple procedure. Often greater differences exist between A(E) obtained by different authors, than existed between the original N'(E) or N(E) data, indicating that different choices for the background or deconvolution procedure introduce the wide variations, rather than the recording of the experimental data or preparation of the sample (Ramaker et al, 1979). We cannot overemphasize the importance of recording the Auger spectrum over a sufficiently wide energy range and then forcing the low energy wing of A(E) to be zero and flat over a 20 to 50 eV energy range. Although this is not always trivial to accomplish, it can be obtained by taking several iterations on the background estimate, and it is the only way of assuring that one is obtaining a reasonable result for A(E) (Ramaker et al., 1979).

The difficulty with extracting A(E) from the experimental data should significantly diminish as new and improved experimental techniques become available. I am particularly hopeful that the new XAES, PAES, and APECS techniques will increasingly provide Auger data without backgrounds, and without damage and charging effects, so that Auger line shape interpretation will become a more common and useful technique for providing electronic structure information on solids.

Basic concepts

Before providing our theoretical framework for quantitatively interpreting the Auger line shapes, we discuss some basic concepts.

The Auger electron has a kinetic energy, E_{kvv}, equal to the difference between the initial core hole state, E_c, and the final two-hole state, $E_v + E_{v'} + U_{vv'}$, thus (Chattarji, 1976),

$$E_{kvv} = E_c - E_v - E_{v'} - U_{vv'}. \qquad (2)$$

In eq. 2, the E's are the corresponding binding energies relative to the Fermi or vacuum level [It makes no difference as long as all binding energies and the kinetic energy is defined relative to the same reference. Often E_{kvv} is measured relative to the vacuum level of the spectrometer and the E's relative to the Fermi level, in which case the work function of the spectrometer, $\varphi \approx 5$ eV, must be subtracted from the right hand side of eq. 2. Unfortunately, in the literature it is often not made clear what the reference is for E_{kvv}.] and U_{vv} is the hole-hole repulsion energy between the final-state holes. U_{vv} can also be referred to as the difference between the first and second ionization potentials.

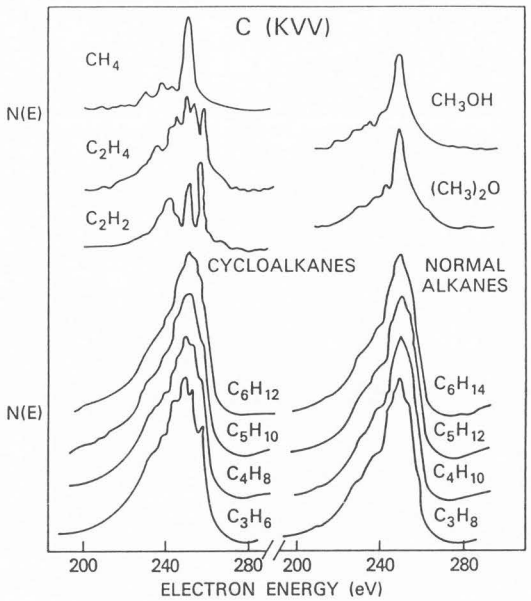

Fig. 2. The C KVV Auger line shapes taken in the gas phase for various carbon molecules as indicated (Rye et al., 1978, 79, & 80).

A basic concept in AES concerns the nature of the density of states (DOS) reflected in the line shape and the localization of the final state holes. Fig. 2 helps illustrate some of these concepts for several gas phase hydrocarbons (Rye et al, 1978,79,80). The sensitivity of AES to local hybridization (sp^3, sp^2, sp) is clearly demonstrated by the CH_4, C_2H_4, and C_2H_2 line shapes. The insensitivity to substituent effects is demonstrated by the CH_4, CH_3OH, and $(CH_3)_2O$ (all sp^3) line shapes. The normal alkanes show a broadened sp^3 line shape. The cyclic alkanes show an apparent progression from the sp^2 to the sp^3 line shape as the bond angle strain decreases. These trends indicate that AES samples a site specific DOS, i.e. the DOS specific to that atom with the initial core hole.

Fig. 2 also shows that the principal peak energy for the alkanes is unchanged in spite of the increasing size of the molecules. This suggests that the final-state holes are not completely delocalized about the molecule in these systems, otherwise $U_{vv'}$ should decrease as the molecule size increases and increase the kinetic energy (Rye et al, 1978,79,80). However, if the holes were completely localized on the methyl group having the initial core hole, we would expect the line shapes to be essentially the same for all alkanes. We will see below that hole-hole

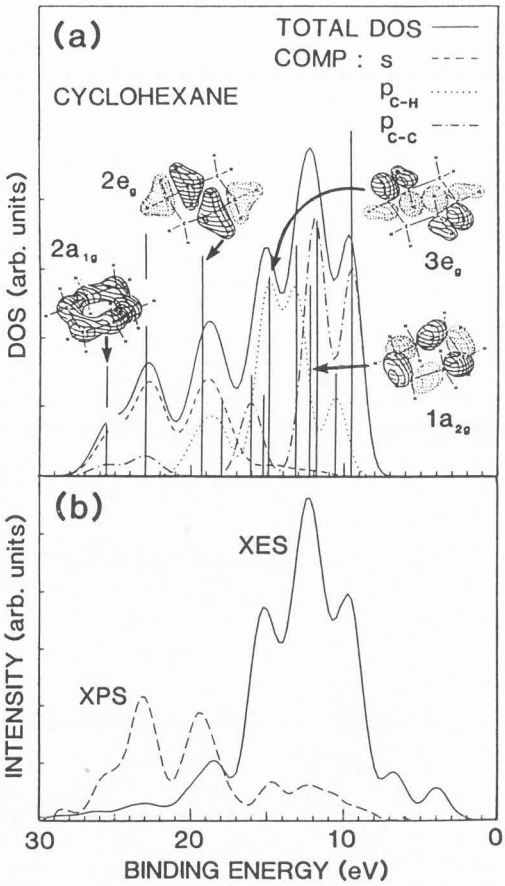

Fig. 3. a) Total one electron DOS (solid line) for cyclohexane determined empirically as described in the text. The s (dashed line), p_{CH} (dotted line), and p_{CC} (dot-dashed line) components, determined as described in the text, are also shown. The vertical lines indicate the electron density on any carbon atom for each MO as obtained from a GAUSSIAN 82 calculation. The energies of each vertical line are placed at those obtained empirically from PES data (Bischof et al., 1969). Schematic diagrams (Jorgensen and Salem, 1973) of four of the molecular orbitals are also given. b) XPS (Mills and Shirley, 1977) and XES (Mattson and Ehlert, 1968) data for cyclohexane as utilized to obtain the DOS in a) above.

correlation or localization distorts the line shape, and for complete localization on a single methyl group, the line shapes for C_nH_{2n+2} ($n > 1$) should be the same as that for CH_4, which clearly is not the case. We will show that although strong correlation effects exist, the holes are believed to be delocalized at least over several methyl groups, if not the whole molecule.

A self-fold of the appropriate one-electron density of states (DOS),

$$\rho * \rho(E) = \int \rho(E-\varepsilon)\rho(\varepsilon)\,d\varepsilon, \qquad (3)$$

is known to represent a first approximation to the line shape (Lander, 1953). The empirical procedure utilized by us for obtaining the DOS has been described previously (Hutson and Ramaker, 1987a). It involves the use of x-ray emission (XES) and photoelectron (XPS) spectra, and in some cases theoretical calculations. Fig. 3 illustrates our procedure for obtaining the DOS for the cyclohexane molecule. The dipole selection rule in the Kα x-ray emission process means that the XES spectrum reflects the p DOS (Mattson and Ehlert, 1968). The Final State Rule (Ramaker, 1982a) also indicates that these DOS reflect those in the final state (i.e. in the absence of the core hole) and not those of the initial state (i.e., in the presence of a core hole.) The Mg Kα XPS spectrum (Mills and Shirley, 1977) reflects primarily the s DOS with a small component of the p DOS (actually s + {1/14}p) (Murday et al, 1981). This small p component can easily be removed from the XPS spectrum to obtain the s DOS. We normalize the XES and XPS spectra to give the well-known sp^3 electron configuration for all the molecules.

Fig. 3a also shows results from a GAUSSIAN 82 calculation (Binkley,1982) which we performed. The indicated energies of the orbitals are not those obtained from the GAUSSSIAN 82 calculation, but rather those from PES data (Mills and Shirley, 1977; Bischof et al., 1969); however, the intensity of each bar is determined by the SCF calculated local DOS on any of the identical carbon atoms in cyclohexane. In general the agreement is reasonable.

Many of the MO's in the alkanes have primarily either carbon-carbon (C-C) or carbon-hydrogen (C-H) bonding character (Jorgensen and Salem, 1973). In the Auger spectrum, it has been shown previously (Jennison,1980) that final states involving these different MO's have different hole-hole repulsions. Therefore, we must separate the p DOS into the p_{CC} and p_{CH} components. We accomplish this by identifying each MO as having either C-C and C-H character upon examining the orbital structure as reported by Jorgensen and Salem (1973). Four such structures are shown in Fig. 3a, showing for example that the $2a_{1g}$ MO has primarily s character, the $2e_g$ has some s and p_{CH} character, and the $3e_g$ and $1a_{2g}$ MO's have p_{CH} and p_{CC} characters, respectively. Using the appropriate identification for each MO, the relative intensities obtained from the GAUSSIAN 82 calculation, and the widths from the semi-empirical DOS, we can separate the total DOS into the s, p_{CC}, and p_{CH} components. The result is shown in Fig. 3a for cyclohexane. Using similar procedures for all of the other molecules, we obtain the required DOS and their components.

For two reasons, we utilize semi-empirically derived DOS, even for simple molecules (Hutson and Ramaker, 1987a). First, most one-electron theoretical calculations do not include electron correlation effects and therefore do not give sufficiently accurate binding energies. Second, the semi-empirical DOS include approximate widths for each orbital feature. Assuming the XES and XPS spectra utilized to obtain the DOS were measured at sufficiently high resolution, these widths primarily reflect broadening due to the vibrational state manifold of the final state which project onto the core initial state in XES, or ground state in PES. $\rho * \rho(E)$ then has twice the broadening consistent with the Auger two-hole

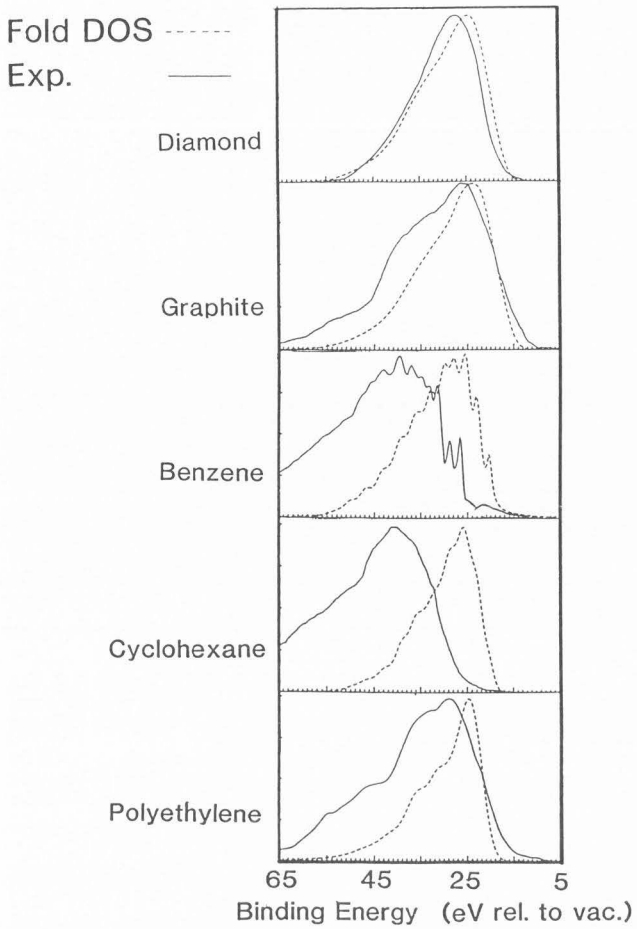

Fig. 4. Comparison of the experimental C KVV Auger line shapes (solid line) obtained from the literature for diamond (Dayan and Pepper, 1984), graphite (Houston et al., 1986), benzene (Siegbahn et al., 1969), cyclohexane (Houston and Rye, 1981), and polyethylene (Dayan and Pepper, 1984; Pepper, 1981) with the self-fold of the DOS (dotted line) obtained as described in the text.

final state.

Fig. 4 compares the DOS self-folds with the experimental Auger line shapes. The Auger line shapes in Fig. 4 for the gas phase hydrocarbons are the raw data (Rye et al., 1978,79,80), those for the solids are obtained from the data (Dayan and Pepper, 1984; Pepper, 1981; Houston and Rye, 1981; Siegbahn et al., 1969) after background subtraction and deconvolution utilizing the procedures described above (i.e. via numerical background removal from N(E)). Fig. 4 reveals several important points. First, note that the experimental line shape for the gas phase molecules is shifted by about 6-10 eV to higher two-electron binding energy (or lower Auger kinetic energy). The binding energy scale is determined by subtracting the Auger kinetic energy from the C K binding energy [i.e. $E_b = -(E_c - E_{kvv})$]. This shift of the experimental line shape to higher binding energy is due to final state hole-hole repulsion, since the two holes cannot completely delocalize. No shift is seen for the solids, since in this case the holes can completely delocalize. However, hole-hole correlation effects are seen in all of the experimental line shapes, as indicated by the clear distortions from the one-electron self-fold. The second interesting point concerns the onset or threshold of the spectra. Although the principal peaks of the gas phase experimental spectra are shifted to higher binding energy, the onsets of both the experimental line shape and the DOS self-fold for each case are essentially the same. This suggests that each of the spectra has at least some contribution which arises from a process producing a final state with a smaller hole-hole repulsion. Furthermore, note that each experimental spectrum extends to much higher binding energy than does the DOS self-fold, indicating a process producing a final state with a higher hole-hole repulsion. We (Hutson and Ramaker, 1987a) have shown that the processes producing these satellite contributions are resonant excitation and initial-state and final-state shakeoff.

We shall refer to these satellites as the ke-vve, ke-v kv-vvv and k-vvv satellites, where the notation indicates the particles in the initial and final states before and after the hyphen. Here, the "k" refers to the initial 1s core hole, the "e" to the resonantly excited bound electron, and v to a valence hole created either by the shakeoff process or by the Auger decay. The principal Auger process is indicated without the hyphen (kvv rather than k-vv) consistent with that used historically. We use kvv to indicate this principal or normal Auger contribution to differentiate it from the total KVV experimental line shape.

In light of the above, the line shape consists of the sum of several contributions; namely,

$$N(E) = c_1 I_{kvv}(E) + c_2 I_{ke\text{-}vve}(E) + c_3 I_{ke\text{-}v}(E) + c_4 I_{kv\text{-}vvv}(E) + c_5 I_{k\text{-}vvv}(E). \quad (4)$$

The process creating each component is illustrated in Fig. 5. Here the ke-vve term refers to the resonant Auger satellite, which arises when Auger decay occurs in the presence of a localized electron, which was created by resonant excitation into an excitonic or bound state upon creation of the core hole. The ke-v contribution arises when the resonantly excited electron participates in the Auger decay. The kv-vvv term is the initial-state shake Auger term arising when Auger decay occurs in the presence of a localized valence hole, which was created via the shakeoff process during the initial ionization. The k-vvv term denotes the final state shake Auger satellite, which arises when Auger decay occurs simultaneously with shakeoff of a valence hole. These latter two terms arise as a direct result of core hole screening. The ke-vve and ke-v terms arise because the Auger process is generally excited by electron excitation which allows the resonant excitation. The coefficients in eq. (2) are obtained by least squares fit to the experimental spectra.

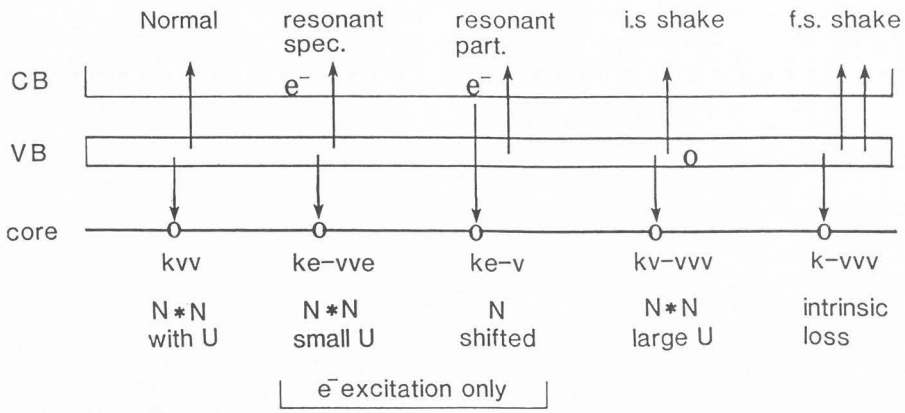

Fig. 5. Summary of the various processes giving rise to the total Auger line shape. Core, VB and CB indicate the core level, valence band (or filled orbitals), and conduction band (or empty orbitals) respectively. Spec. (spectator) and part. (participant) indicate the subsequent fate of the resonantly excited electron during the Auger process. I.s and f.s. indicate initial-state and final-state and refer to the state in which the shakeoff event occurs relative to the Auger decay. N*N and N (N = ρ in eq. (6))refer to the approximate line shape, i.e. either a DOS self-fold, or just the DOS, with the relative size of DU in the Cini expression (eq. 6) indicated. The resonant satellites occur only under electron excitation.

Theoretical framework

The principal kvv line shape

Our theoretical prescription (Hutson and Ramaker, 1987a) for generating the kvv term can best be expressed by the equation,

$$I_{kvv}(E) = B \Sigma_{ll'}[P_{kll'} R_l R_{l'} A(E+\delta_{\lambda\lambda'},\Delta U_{\lambda\lambda'},\rho_l,\rho_{l'})]. \quad (5)$$

The Cini-Sawatzky function (Cini, 1977,78; Sawatzky, 1977),

$$A(E, \Delta U, \rho, \rho') = \frac{\rho * \rho'(E)}{[1-\Delta U\ I(E)]^2 + [\Delta U\ \pi\ \rho * \rho'(E)]^2} \quad (6)$$

introduces hole-hole correlation effects, and distorts the DOS self-fold. Here ΔU is the effective hole-hole correlation parameter and I(E) is the Hilburt transform,

$$I(E) = \int \rho(\varepsilon)/(E-\varepsilon)\, d\varepsilon. \quad (7)$$

The Cini function, which distorts the DOS self-fold for treatment of Auger line shapes in solids, mimics the effects of configuration interaction theory on the DOS for molecules (Hutson and Ramaker, 1987a; Ramaker, 1980). Thus it can be used (albeit with some modifications) on the DOS self-fold for molecules as well. In eq.(5) we have included additional arguments in A to make explicit the point that the total theoretical kvv line shape is a sum of components, with each ll' component (e.g. the ss, sp, and pp components) having an energy shift, $\delta_{\lambda\lambda'}$, and a hole-hole correlation parameter, $\Delta U_{\lambda\lambda'}$, and with each component derived from a fold of the ρ_l and $\rho_{l'}$ DOS (e.g. s or p) as defined in Fig. 2. The subscripts λ are defined below. The atomic Auger matrix elements $P_{kll'}$ (normalized per electron) are obtained from experimental and theoretical results for neon (Ramaker, 1985; 1982b). The relative magnitudes utilized in this work are P_{css} = 0.8, P_{csp} = 0.5, and P_{cpp} = 1. as reported previously (Ramaker, 1985). In eq.(5), B is a normalization constant and the R_l are core hole screening factors defined as below.

We have shown previously (Ramaker, 1980, Dunlap et al., 1981) that in covalent systems, intermediate levels of localization can occur. As ΔU increases relative to the effective covalent interaction, the holes localize first from the bond or molecular orbital to a "cluster" orbital, and then to a bond orbital. A simple examination of the MO's for the alkanes or diamond (Jorgensen and Salem, 1973) suggests strongly that the appropriate local orbital for these carbon based systems is the tetrahedral cluster orbital involving four sp^3 bond orbitals surrounding a single C atom (i.e. a methyl-like group). Similarly, for the alkenes or graphite, the appropriate local orbital is the sp^2 cluster for the σ bonds, and a single p orbital for the π bonds. In light of the above, the ΔU's can be interpreted in this work as the difference between the hole-hole repulsion when two holes are localized on the same local cluster orbital (U_{11}) verses when they are localized on different neighboring cluster orbitals (U_{12}). The δ parameters can be interpreted as the repulsion energy when the holes are completely delocalized about the system (Hutson and Ramaker, 1987a). They remain finite for molecules, and are zero for the extended covalent solids (See further discussion of this point in the Summary below).

The subscripts λλ' in eq. (5) on the ΔU and δ parameters are to make explicit that these parameters vary with the nature of the orbital combination. Thus for the alkanes we allow three different ΔU's, namely for the CH-CH, CH-CC, and CC-CC σ orbital combinations, and for the alkenes three different ΔU's, namely for the σσ, σπ, and ππ orbital combinations. With this prescription, the separate ss, sp, and pp angular momentum contributions to the Auger line shape, which

belong to the same $\lambda\lambda'$ contribution, are required to have the same ΔU and δ parameters. There are generally six different ll' contributions, but we allow only three different ΔU and δ parameters for each molecule, and these are determined to provide optimal agreement with experiment (Hutson and Ramaker, 1987a & b; Houston et al., 1986; Ramaker and Hutson, 1987).

The factors R_l in eq. (5) are to make our theory consistent with the previously derived final state rule for Auger line shapes (Ramaker, 1982a). The final state rule indicates that 1) the shape of the individual ll' contributions should reflect the DOS in the final state, and 2) the intensity of each ll' contribution should reflect the electron configuration of the initial state. For the kvv line shape, the final state is without the core hole. We assume that the DOS in the final state and ground state are similar, so the spectral shape of ρ_l should reflect the ground DOS. However, the initial state in the kvv process has a core hole, therefore the integrated ρ_l should reflect the electron configuration of the initial core hole (CHS) state. The R_l factors are defined,

$$R_l = \int \rho_{CHS,l}(\varepsilon)d\varepsilon \Big/ \int \rho_l(\varepsilon)d\varepsilon . \qquad (8)$$

In this work we assume all R_l are similar so that they can be ignored. Effectively this ignores the "static" effects of core hole screening; the shakeoff contributions are "dynamic" core hole screening effects which are included.

The satellites

The ke-vve and kv-vvv satellites are also generated by eq. (5) but with different values for $\Delta U_{ll'}$ and $\delta_{ll'}$ (Hutson and Ramaker, 1987a). For the ke-vve satellite the spectator electron can screen the two holes and reduce the repulsion. We assume that $\Delta U_{ll'}$ is zero (i.e. no distortion due to correlation occurs), and determine $\delta_{ll'}$ empirically for optimum fit to experiment. Of course $\delta_{ll'}$ should be smaller than for the kvv case. For the kv-vvv satellite, the three hole final state experiences a larger effective repulsion. We have shown previously (Hutson and Ramaker, 1987a & b) that it is twice that for the kvv term if the shake hole is localized on the methyl group or atom with the core hole, and equal to that for kvv if it is delocalized throughout some larger subcluster of the molecule. Of course in the solid, no kv-vvv satellite appears if the shake hole completely delocalizes. $\delta_{kv\text{-}vv'v''}$ is again determined empirically and should be larger then for δ_{kvv}.

The ke-v satellite can be generated from eq. (5) assuming that the sum over l' is limited to the orbital with the resonantly excited electron (Hutson and Ramaker, 1987a). Again ΔU is zero, since a single hole exists in the final state, and $\delta_{ll'}$, determined empirically, is equal to the exciton binding energy. The k-vvv satellite is generated by the Bethe expression, $\log(E/E_{th})/(E/E_{th})^m$ for $E>E_{th}$ (Ramaker et al, 1979; Hutson and Ramaker, 1987a). E_{th} is a parameter representative of the threshold energy for intrinsic loss, and m is a parameter usually around one.

The basic processes for C_2H_4/Ni are different from that for the others, but they can

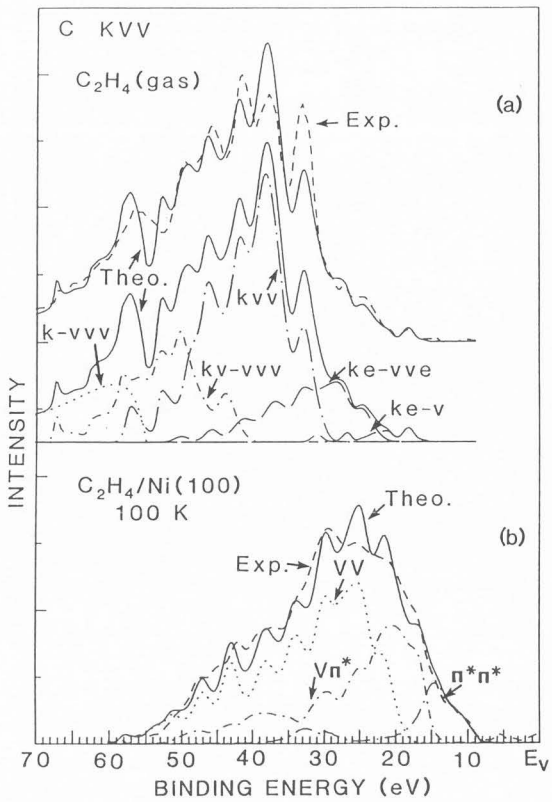

Fig. 6. a) Comparison of the C KVV experimental (Rye et al., 1978, 79, & 80) and theoretical (Hutson and Ramaker, 1987a) Auger line shapes for ethylene gas. The various contributions (kvv, kv-vvv, k-vvv, ke-v, ke-evv) were obtained as described in the text. b) Comparison of the experimental (Koel, private communication) and theoretical (Hutson, Ramaker, and Koel, to be published) Auger line shapes for ethylene chemisorbed on Ni(100) at 100 K (π-bonded ethylene). The three components (VV, Vπ^*, $\pi^*\pi^*$) line shapes were obtained as described in the text. The relative intensities were obtained by least squares fit to the experimental data.

be related to the gas phase molecular case (e.g. ethylene) (Hutson, Ramaker, and Koel, to be published) . The spectrum in Fig. 6b was excited by x-rays, so that no resonant satellites should appear (B. Koel, private communication). However, charge transfer from the substrate into the π^* orbital occurs to screen the holes, in both the core-hole initial state and the two- or three-hole Auger final state. This charge transfer has the affect of decreasing the ΔU and δ parameters; the transferred charge playing the role of the resonantly excited electron in the gas phase (Hutson, Ramaker, and Koel, to be published). Thus the kvv and kv-vvv contributions which comprise the intramolecular component (i.e. termed the VV component) for the chemisorbed state are similar to the ke-vve and kvv in the gas. The Vπ^* component is similar to the ke-v, and the $\pi^*\pi^*$ component is a new

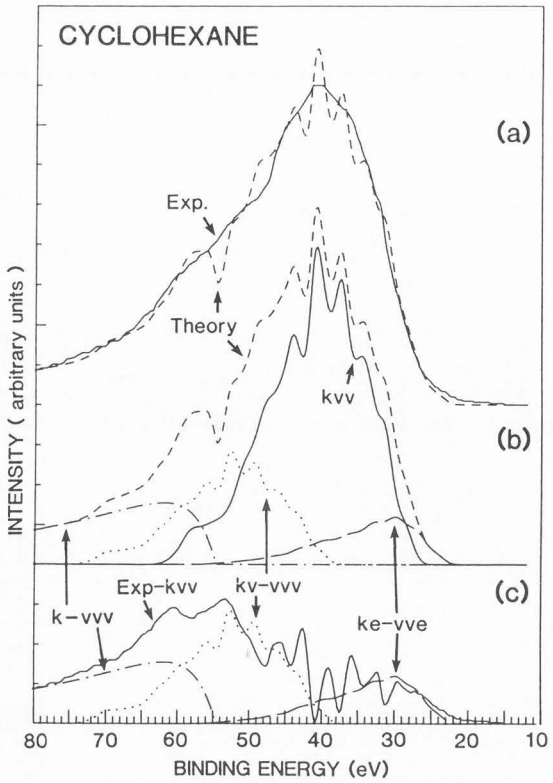

Fig. 7. a) Comparison of the experimental C KVV line shape for cyclohexane (Houston and Rye, 1981) with the total theoretical line shape (Hutson and Ramaker, 1987a) obtained as described in the text. b) The total theoretical line shape and each of the components as indicated. c) Comparison of the satellite components with the difference spectrum (experimental - theoretical kvv component).

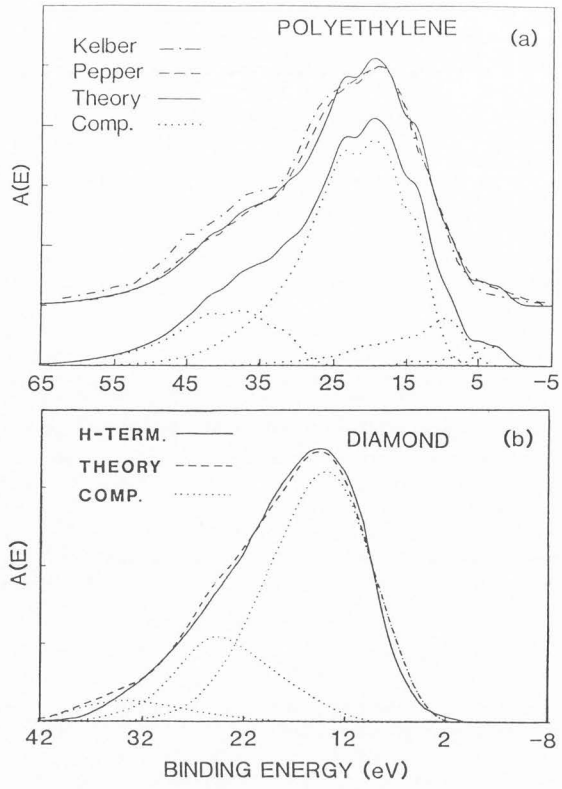

Fig. 8. a) Comparison of the experimental Auger line shape for polyethylene from Kelber et al (1982) and Dayan and Pepper (1984)) with the theoretical total line shape (Hutson and Ramaker, 1987b) determined as described in the text. The components in order of increasing energy are kv-vvv, kvv, ke-vve, and ke-v. b) The C KVV Auger line shapes for the H terminated (Dayan and Pepper, 1984) surface of diamond. The A(E) line shape results after the background subtraction and deconvolution procedures. The H-terminated line shape is more representative of the bulk since C-H bonds are more similar to bulk C-C bonds than the π bonds existing in the clean surface. Also shown is a comparison of the H terminated line shape with the theoretical kvv line shape (Ramaker and Hutson, 1987) determined as described in the text. The s*s, s*p, and p*p components have maxima at 248, 258, and 268 eV, respectively.

contribution unlike that of any in the gas phase, in fact it is approximated in Fig 6b by the Ni L_3VV Auger line shape. Although the latter two components are facilitated through an intra-atomic $V\pi^*$ and $\pi^*\pi^*$ Auger process, respectively, they ultimately appear inter-atomic in character because one or both holes ultimately end up on the substrate.

Application to the C KVV line shapes

Figs. 6-8 compare the optimal theoretical line shape and each of the components with the experimental line shapes for ethylene (Rye et al., 1978,79, & 80), ethylene/Ni (Koel, private communication), cyclohexane (Siegbahn et al, 1969), polyethylene (Dayan and Pepper, 1984; Kelber et al., 1982), and diamond (Dayan and Pepper, 1984; Lurie and Wilson, 1977). In general the theoretical line shapes generated by the prescription above agrees nicely with the experimental line shapes. Similarly good agreement is obtained for the systems not shown, i.e. for methane, ethane, benzene, and graphite (Hutson and Ramaker, 1987a, Houston et al., 1986). Table 1 summarizes the ΔU and δ parameters for the principal kvv components, and Table 2 the results for the satellites.

The kvv component

Table 1 reveals that for the alkanes the ΔU's are larger for the CH MO's than for the CC MO's. This can be understood simply from the more localized character of a CH orbital about a single C atom (increased U_{11}), and decreased interaction between CH cluster orbitals (decreased U_{12}), compared with CC cluster orbitals (Jorgensen and Salem, 1973). Likewise for the alkenes, contributions involving only the π MO's have a zero ΔU. This is consistent with one's chemical intuition concerning the de-localized π orbitals and also consistent with that found

Table 1 Summary of ΔU and δ parameters obtained empirically for the theoretical kvv line shape.[a]

Molecule	ΔU (eV)			δ[b] (eV)		
Alkanes	CH-CH	CH-CC	CC-CC	CH-CH	CH-CC	CC-CC
Methane	0			12		
Ethane	1	1	0	12	10	10
Cyclohexane	3	3	1.25	9	9	9
Polyethylene	3	3	1.25	0	0	0
Diamond			2.			0
Alkenes	σσ	σπ	ππ	σσ	σπ	ππ
Ethylene	2	1	0	9	11	11
Benzene	2	1	0	8	6	6
Graphite	2	1	0	0	0	0

[a]From Ramaker and Hutson (1987a).
[b]A positive δ indicates a shift to higher two-hole binding energy.

previously for graphite. Generally within a single molecule the ΔU's decrease in the order σσ>σπ>ππ for the alkenes, and CH-CH > CH-CC > CC-CC for the alkanes as expected.

Note that the ΔU's for the CH-CH orbital in methane and for the CC-CC orbital in ethane are zero. This is by design (Hutson and Ramaker, 1987a). Since only one of these cluster orbitals exist for each molecule, no CI distortion effects (at least of the type included by the Cini expression) are expected for these contributions. Since at least two CH orbitals exist in ethane, the CH-CH and CH-CC contributions have non-zero ΔU's.

Multiplet effects are becoming large in the smaller molecules, such as methane, ethane and ethylene. This is particularly evident in the ethylene spectrum. The two peaks between 30 and 40 eV in the theoretical kvv line shape have widely different intensity, however in the experimental spectrum they have similar intensity (see Fig. 6). We have shown previously (Hutson and Ramaker, 1987a) that this arises because of multiplet splitting which is absent in our theory

Comparison of the ΔU's between molecules indicates something about the nature of the screening processes in these molecules. Note that the ΔU for the CC-CC contribution increases in the order cyclohexane < polyethylene < diamond. This can be understood from the definition of $\Delta U = U_{11} - U_{12}$. For very short screening lengths, one might expect both U_{11} and U_{12} to be reduced substantially, so that ΔU would be decreased (Houston et al., 1986). For long screening lengths, one might expect U_{12} to be decreased more than U_{11}, having the effect of increasing ΔU. We believe that the latter is occurring in the current systems. The longer chain length in polyethylene and full three dimensional covalency in diamond suggests that the extent of polarization should increase in the order cyclohexane < polyethylene < diamond. This increased polarization then has the effect of increasing ΔU. For the alkenes, the DU's are all the same. This suggests that the screening length is much shorter so that "full" screening already occurs in ethylene. This is consistent with the more delocalized π electrons in the alkenes.

The variation of the δ parameter is not as systematic as that found for ΔU; nevertheless, some important trends are evident. We can interpret the δ's as the delocalized molecular hole-hole repulsion (Hutson and Ramaker, 1987a; Dunlap et al, 1981). As the size of the molecule increases, δ decreases, reflecting the ability of the two final state holes to stay apart from each other in the delocalized molecular orbitals. Note also that for similar sized molecules, the δ's for the alkenes are smaller than for the alkanes. This may reflect the increased screening due to the π electrons.

The resonant satellites

Resonant satellites are present in the polyethylene line shape (Hutson and Ramaker, 1987b), but not in diamond or graphite (Ramaker and Hutson, 1987a; Houston et al., 1986). This is because polyethylene has an excitonic level as seen by x-ray absorption (XAS) (Seki et al, 1977) and electron energy loss (EELS) (Ritsko, 1979) data. In diamond and graphite, no such excitonic level exist so that the resonantly excited electron does not remain as a spectator or participator in the Auger decay (Morar et al., 1985). In small molecules, the resonantly excited electron cannot escape, so that under electron excitation, resonant satellites are expected. Similar resonant satellites have in fact been observed in XES spectra (Mattson and Ehlert, 1968; Nordgren et al., 1983).

Table 2 summarizes the resonant satellites as characterized by their relative intensities and energy shifts, $\delta_{ke\text{-}v}$ and $\delta_{ke\text{-}vve}$. Note that the ke-vve intensities are all around 6-13% and the ke-v less than 3%. The intensities of the resonant satellites depend on the electron excitation energy and the secondary cascade process, so that their absolute intensities are not very interesting. It should be pointed out, however, that by utilizing synchrotron radiation tuned to the exact resonant energy, one could obtain experimentally just the resonant contributions (Chen et al., 1985). This process has been called de-excitation electron spectroscopy (DES), and has been reported for both gas phase and chemisorbed CO, where the $2\pi^*$ level is resonantly populated.

Table 2 Summary of satellite characteristics.[a]

ke-v	Rel. Int(%)	ΔU(eV)	δ[c](eV)	E_e+U_{ce} (eV)
Ethylene	2.	0	7.	6.3
Benzene	1.	0	5.	5.1
[b]Ethylene/Ni ($V\pi^*$ comp)	27	0	0	-
ke-vve				**Δδ**
Methane	12.	0	7.	5.
Ethane	12.	0	8	4
Cyclohexane	8.	0	4.	5.
Polyethylene	11.	0	-5.	5.
Ethylene	13.	0	3.	7.
Benzene	6.	0	-1.	8.
[b]Ethylene/Ni (VV comp)	45	0	0	-
kv-vvv				**$\delta_{(CH-CH)}$ (eV)**
Methane	20.	0	$\delta_{kvv}+5$	17
Ethane	21.	ΔU_{kvv}	$\delta_{kvv}+5$	17
Cyclohexane	19.	ΔU_{kvv}	$\delta_{kvv}+11$	20
Polyethylene	17.-21.	ΔU_{kvv}	18	18
Ethylene	20.	$2\Delta U_{kvv}$	$2\delta_{kvv}$ 18	
Benzene	21.	$2\Delta U_{kvv}$	$2\delta_{kvv}+4$	20
[b]Ethylene/Ni (VV & $V\pi^*$)	20	ΔU[d]	$\delta_{kvv}+5$[d]	14
k-vvv	**Rel. Int (%)**	**E_{th}(eV)**	**kvv Int.(%)**	
Methane	17.	53	53.	
Ethane	15.	50	49.	
Cyclohexane	19.	53	50.	
Polyethylene	0		70.	
Ethylene	15.	50	54.	
Benzene	16.	50	54.	

[a]From Ramaker and Hutson (1987a).
[b]The characteristics of the π^*V and VV components of the primary kvv term for ethylene/Ni are also indicated because these resemble the satellite line shapes for ethylene gas.
[c]A positive δ indicates a shift to higher two-hole binding energy.
[d]The ΔU and δ indicated here are that for gas phase ethylene.

Although their individual intensities are not of interest, the ratio of intensities, I(ke-v)/I(ke-vve), indicates something about the character of the excitonic level. The atomic Auger matrix elements per electron are essentially the same, for the ss, sp and pp contributions in kvv spectra (Houston et al., 1986). Therefore, we can estimate what the ratio of intensities should be, based purely on the ratio of local electron densities, assuming a completely localized excitonic level. With an initial state charge distribution of $\sigma_s\sigma_p^2\pi e$, I(ke-v)/I(ke-vve) should be 0.5, compared with ≈0.14 for the alkenes found experimentally. This suggests that although the excitonic level may be localized in time, it must be of a more diffuse nature spatially. The factor of two or more reduction from that expected theoretically suggests that the excited electron spends only part of its time on the methyl group with the core hole, the other part of the time presumably on neighboring carbon atoms or methyl groups.

Table 2 also summarizes the required shifts, δ_{ke-v} and δ_{ke-vve} for the resonant satellites. δ_{ke-v} should be equal to the binding energy of the excitonic electron. We compare δ_{ke-v} with the binding energies obtained from EELS data (Hitchcock and Brion, 1977) in Table 2. Good agreement between these two results is obtained.

The shifts δ_{ke-vve} vary over a large range, although these shifts are much larger for the alkanes than for the alkenes. This reflects the greater screening of the final state holes by an electron in a π^* orbital compared with that in a diffuse Rydberg orbital. The difference in shifts,

$$\Delta\delta = \delta_{kvv} - \delta_{ke-vve} = 2U_{ve} - U_{ce} \qquad (9)$$

should directly reflect the nature of the core, U_{ce}, and valence, U_{ve}, polarization energies (Hutson and Ramaker, 1987a & b). These are tabulated in Table 2. We see that Δδ is generally about 5 eV for the alkanes and 8 ev for the alkenes.

The shakeoff satellites

We note that the relative intensities of the

kv-vvv satellites for the 6 molecules listed in Table 2 are essentially all around 20% to within experimental error. This is in contrast to graphite (Houston et al., 1986) and diamond (Ramaker and Hutson, 1987a), which indicated no initial state shake satellites. The absence of such satellites in graphite and diamond arises because the shake hole in the initial state of these covalently bonded solids does not stay localized near the core hole for a time sufficient to "witness" the Auger decay. We have shown elsewhere (Hutson and Ramaker, 1987b) that in the presence of a core hole, the occupied valence band DOS of diamond indeed does not exhibit any bound states. On the other hand, the DOS for polyethylene in the presence of a core hole does exhibit narrow peaks indicative of bound-like states, consistent with the initial state shake/Auger satellite observed.

Methane is isoelectronic with the neon atom. The shakeoff probability for neon has been both measured and calculated to be around 21% (Carlson et al., 1975 & 1968; Ramaker and Murday, 1979), in excellent agreement with that found for all of the carbon systems in this work. This agreement provides further empirical evidence for the validity of the methyl sub-unit orbital pictured in these carbon systems.

Column 3 of Table 2 shows that the most appropriate ΔU for the kv-vvv satellite is the same as that for the kvv line shape in the alkanes, but twice that for the kvv line shape in the alkenes. This means that for the alkenes, the shake hole is localized primarily on the methyl group with the core hole , but in the alkenes the shake hole is more delocalized onto some sub-cluster of the alkane chain (Hutson and Ramaker, 1987b). We attribute this different behavior to the different polarization lengths in the alkanes and the alkenes. In the alkenes, the π electrons screen the core hole, reducing the polarization potential which neighboring methyl groups experience. Thus the neighboring methyl groups remain in the band and the shake hole stays localized on the primary methyl group containing the core hole. In the alkanes, the core hole potential "pulls down" not only the primary methyl group, but the neighboring methyl groups are partially "pulled down" as well, enabling the shake hole to partially delocalize over the neighboring methyl groups (Hutson and Ramaker, 1987b).

Finally, in columns 4 and 5 of Table 2, we consider the optimal shifts, $\delta_{kv\text{-}vvv}$, of the theoretical kv-vvv satellite. Column 4 indicates how the kv-vvv satellite was generated. For the alkanes, the kv-vvv line shape has exactly the same shape as the kvv line shape and it is simply shifted down by an amount $\delta_{kv\text{-}vvv}$-δ_{kvv}. For the alkenes, the $\delta_{kv\text{-}vvv}$ shifts are generated by doubling the δ_{kvv} shifts, consistent with the doubling of the ΔU's. For benzene, an additional shift of 4 eV was added to provide optimal agreement with experiment (Hutson and Ramaker, 1987a). Column 5 gives the total shift relative to the one-electron picture for the major CH-CH bonding contribution. Column 5 reveals no systematic change in δ(CH-CH), indeed to within experimental error, it is essentially constant. This is in contrast to the δ_{kvv} tabulated in Table 1, where we see that as the molecules get larger, the δ_{kvv} decrease for both the alkanes and alkenes. We conclude that in the three-hole final state of the kv-vvv process, the three holes are consistently localized on some sub-cluster of the molecule (i.e., a methyl group), whereas in the kvv process, the two-holes are delocalized throughout the molecule (Rye et al., 1978, 79, 80, & 88). Again we see, that the larger the repulsive forces, the more localized the final state holes, consistent with the Cini theory (Cini, 1977,78).

Table 2 shows that the empirically determined intensity for the k-vvv satellite is quite constant around 17%. This intensity was determined by integrating the area under the Bethe expression (Hutson and Ramaker, 1987a) from E_{th} down to E_{th} + 50 eV. This includes most of the final state shake satellite although some intensity exist beyond this region. This could easily introduce an error of 3%, so that to within experimental error, the initial and final state satellite intensities are similar, as expected.

Summary

We summarize the results as follows:

1) The normal kvv line shape accounts for only about half of the total experimental intensity for the gas phase molecules. This is in contrast to polyethylene where it accounts for 70%, and in diamond and graphite where it accounts for 100%.

2) The remaining part of the experimental intensity can be attributed to 3 different satellite contributions; namely resonant excitation, initial-state-shake, and final-state shake satellites (i.e. via ke-vve, kv-vvv, and k-vvv processes).

3) In contrast to that reported previously (Rye et al., 1978, 79, 80, 88), the normal kvv Auger line shapes reflect delocalized holes (at least over 3 or more methyl groups), but correlation effects are evident. In contrast, the 3-hole final state of the kv-vvv process reflects holes localized primarily on a single methyl group.

4) The ΔU's of the kvv line shape for the gas phase molecules and the solids are similar, indicating long range screening effects are not important. On the other hand, the kvv and kv-vvv line shapes reveal that π electron screening within the alkenes is important.

5) Perhaps the most important result, the chemical effects seen in the line shapes do not arise from one-electron effects, but rather from many-body correlation effects. Thus the differences seen between graphite and diamond result because diamond has just the σ orbitals with a single ΔU, graphite has both σ and π orbitals with differing ΔU's for the $\sigma\sigma$, $\sigma\pi$, and $\pi\pi$ holes. On the other hand, since hole-hole correlation and repulsion effects are much diminished for chemisorbed systems because of metallic screening from the substrate, in the chemisorbed case, and only in this case, the C KVV Auger line shape reflects the DOS self-fold without significant distortion.

We note here that some controversy exists

over the third conclusion above. Previously Rye and co-workers (Rye, 1978, 79, & 80) concluded that even the normal kvv line shapes for the hydrocarbons reflected localized holes (i.e. on a single methyl group). This conclusion was based on the qualitative energy alignment of the principal peak in the Auger line shapes for the alkane series C_nH_{2n+2} (n = 1 to 6) as seen in Fig. 2. We, however, attribute this to the constant nature of the sum $\Delta U + \delta$ as seen in Table 1 (this sum remains at 12 eV for methane through cyclohexane). The effects of δ is to move the entire line shape to higher binding energy; the effect of ΔU is to distort the line shape so that the peak moves to higher two-hole binding energy. Thus the peak energy remains constant, but the line shape changes upon going from methane, to ethane, to cyclohexane.

We note that some controversy also exists over the magnitude of δ for polyethylene. Within the theory utilized above, we might expect that δ should be zero for an infinitely long covalently bonded chain. However, Rye (1989) after careful determination of the Fermi level, has recently reported that the lineshape for polyethylene is shifted downward by about 10 eV. More extensive work by Turner et al (N.H. Turner, D.E. Ramaker, and F.L. Hutson, to be published), utilizing a more rigorous method to determine the Fermi level, suggests that this shift is more like 1 ± 1 eV (i.e. the uncertainties in the data make it impossible to determine if a shift actually occurs, and if it occurs it is definitely much less than 10 eV). We note that we cannot rule out a shift on a theoretical basis. A non-zero δ could mean that the delocalization process is relatively slow in a one-dimensional chain compared to escape of the Auger electron. Since the avenues for escape are more limited than in a three dimensional system, this could explain why δ could be non-zero for polyethylene but zero for diamond and graphite. This is a very interesting conjecture, but obviously more experimental and theoretical work is required before any definite conclusions can be reached on this point.

Finally, the nature of the hole-hole localization is important to an understanding of damage or dissociation of various hydrocarbon molecules or carbon based solids. The well-known Knotek-Feibelman (1978) mechanism suggests that desorption from a surface is often initiated by Auger decay. In these covalent systems, the desorption or molecular dissociation is believed to occur as a result of a Coulomb explosion, which is of course enhanced when the holes are localized on a sub-cluster of the molecule (Ramaker, 1981). In light of this, the third conclusion above concerning localization of 3-holes on a single methyl group would suggest that shake-off is indeed very important to the damage or molecular dissociation process.

Since it is clear from this work that chemical effects in the Auger spectra arise primarily from the complex many-body effects (i.e. hole-hole correlation and screening) and not from the simple one-electron DOS self-folds, it remains a challenge to extract the chemical bonding information. Nevertheless, we have described here a generally applicable, semi-empirical approach for quantitatively interpreting the Auger line shapes, and thus a relatively straightforward procedure for gaining significant and detailed information about electron delocalization and correlation, screening effects, bonding, and hybridization from Auger line shapes. We anticipate further application of these procedures in the future.

Acknowledgment Supported in part by the Office of Naval Research.

References

Bader SD, Richter L, and Brodsky MB. (1981). Silicon $L_{23}VV$ Auger line shapes and oxygen chemisorption study of Pd_4Si. Solid State Commun. 37, 729-732.

Binkley JS, Frisch M, Raghavachari K, Defrees D, Schlegel HB, Whiteside R, Fluder E, Seeger R, and Pople JA. (1982). Gaussian 82, Release H computer code, Carnegie-Mellon University.

Bischof P, Hashmall JA, Heilbronner E, and Hornung V. (1969). Photoelectron spectroscopic determination of the correlation energy in conjugate double bonds. Helv. Chim. Acta 52, 1745-1749.

Carlson TA. (1975). The nature of secondary electrons created as the result of electron shakeoff and vacancy cascades. Radiat. Res. 64, 53-69.

Carlson TA, Nestor Jr. CW, Tucker TC, and Malik FB. (1968). Calculation of electron shakeoff for elements from Z=2 to 92 with use of self consistent field wavefunctions. Phys, Rev. 169, 27-36.

Chattarji D. (1976). The Theory of Auger Transitions (Academic Press, NY), p. 192.

Chen CT, DiDio RA, Ford WK, Plummer EW, and Eberhardt W. (1985). Dynamics of adsorbate core-hole decay. Phys. Rev. B32, 8434-8437.

Cini M. (1977). Two hole resonances in the XVV Auger spectra of solids. Solid. State Commun. 20, 681-84.

Cini M. (1978). Comment on quantitative Auger spectra in narrow band metals. Phys. Rev. B17, 2788-2789.

Dayan M and Pepper SV. (1984). Study of the Auger line shape of polyethylene and diamond. Surf. Sci. 138, 549-560.

Dunlap BI, Hutson FL, and Ramaker DE. (1981). Auger Line shapes of Solid Surfaces - Atomic, Bandlike, or Something Else?. J. Vac. Sci. Technol. 18, 556-560.

Fuggle JC. (1981). Electron Spectroscopy: Theory, Technique and Applications, Vol 4, Brundle CR and Baker AD eds., (Academic Press, NY), p.85.

Haak HW, Sawatzky GA, and Thomas TD. (1978). Auger-photoelectron coincidence measurements in copper. Phys. Rev. Letters 41, 1825-1827.

Haas TW, Grant JT, and Dooley GJ. (1972). Chemical effects in Auger electron spectroscopy. J. Appl. Phys. 43, 1853-1860.

Hitchcock AP and Brion CE. (1977). The ultraviolet photoelectron spectra of aliphatic and aromatic compounds. J. Electron. Spectrosc. Related Phenom. 10, 317-327.

Houston JE, Rogers JW, Rye RR, Hutson FL, and Ramaker DE. (1986). Relationship between the Auger line shape and the electronic properties of graphite. Phys. Rev. B34, 1215-12

Houston JE and Rye RR. (1981). Auger electron spectra of cycloalkanes C_3 through C_6. J. Chem. Phys. 74, 71-76.

Hutson FL and Ramaker DE. (1987a). Identification of Resonant Excitation and Shakeoff Contributions to the C KVV Auger Line shapes of Several Gas Phase Hydrocarbons. J. Chem Phys. 87, 6824-6837.

Hutson FL and Ramaker DE. (1987b). Identification of Satellites due to Resonant Excitation and Shakeoff in the C KVV Auger Line shape of Polyethylene. Phys. Rev. B35, 9799-9804.

Jennison DR, (1980). The calculation of molecular and cluster Auger spectra. Chem. Phys. Letters 69, 435-46.

Jorgensen WL and Salem L. (1973). The Organic Chemists Book of Orbitals (Academic, New York).

Kelber JA, Rye RR, Nelson GC, and Houston JE. (1982). Auger spectroscopy of polyethylene and polyethylene oxide. Surf.Sci. 116, 148-162.

Knotek ML and Feibelman PJ. (1978). Ion desorption by core-hole Auger decay. Phys. Rev. Letters 40, 964-967.

Lander JJ. (1953). Auger peaks in the energy spectra of secondary electrons from various materials. Phys. Rev. 91, 1382-1387.

Lurie PG and Wilson JM. (1977). The diamond surface. I) The structure of the clean surface and the interaction with gases and metals. Surf. Sci. 65, 453-475.

Madden HH and Houston JE. (1976). Correction of distortions in spectral line profiles: applications to electron spectroscopies. J. Appl. Phys. 47, 3071-3082.

Madden HH and Houston JE. (1977a). Auger electron spectroscopic investigation of the transition density of states from lithium. Solid State Commun. 31, 1081-1087.

Madden HH and Houston JE. (1977b). KVV Auger spectrum of oxidized lithium. J. Vac. Sci. Technol 14, 412-415.

Mattson RA and Ehlert RC. (1968). Carbon characteristic x-rays from gaseous compounds. J. Chem. Phys. 48, 5465-5470.

Mills BE and Shirley DA. (1977). X-ray photoemission spectra of the 2s valence orbitals in cylic alkanes in relation to valence bands of amorphous group 4 and 5 elements. J. Am. Chem. Soc. 99, 5885-5888.

Morar JF, Himpsel FJ, Hollinger G, Hughes G, Jordan JL. (1985). Observations of the C 1s exciton in diamond. Phys. Rev. Letters 54, 1960-1963.

Mularie WM and Peria WT. (1970). Deconvolution techniques in Auger electron spectroscopy. Surf. Sci. 26, 125-141.

Murday JS, Dunlap BI, Hutson FL, and Oelhafen P. (1981). Carbon KVV Auger line shapes of graphite and stage-one cesium and lithium intercalated graphite. Phys. Rev. B24, 4764-4770.

Nordgren J. Selander L, Pettersson L, Brammer R, Backstrom M, and Nordling C. (1983). Electronic structure of benzene studied in ultra-soft x-ray emission. Phys. Scripta 27, 169-1171.

Pepper SV. (1981). Electron spectroscopy of the diamond surface. Appl. Phys. Lett. 38, 344-346.

Ramaker DE, Murday JS, and Turner NH. (1979). Extracting Auger Line shapes from Experimental Data. J. Electron. Spectrosc. Related. Phenom. 17, 45-65.

Ramaker DE and Murday JS. (1979). Factors Contributing to the Si $L_{23}VV$, Si $L_1L_{23}V$ and O KVV Auger Line shapes in SiO_2. J. Vac. Sci. Technol. 16, 510-513.

Ramaker DE. (1980). Final State Correlation Effects in Auger Line shapes, Application to Silicon Dioxide. Phys. Rev. B21, 4608-4623.

Ramaker DE, White CT, and Murday JS. (1981). Auger induced desorption of covalent and ionic systems. J. Vac. Sci. and Technol. 18, 748-752.

Ramaker DE. (1982a). A Final State Rule for Auger Line shapes. Phys. Rev. B25, 7341-7351.

Ramaker DE. (1982b). "Auger Spectroscopy as a Probe of Valence Bonds and Bands" in Chemistry and Physics of Solid Surfaces IV, Vanselow R and Howe R, eds. (Springer, Berlin) p. 19-49.

Ramaker DE. (1985). Bonding Information from Auger Spectroscopy. Applic. Surf. Sci. 21, 243-267.

Ramaker DE and Hutson FL. (1987). Direct Experimental Evidence for Antiferromagnetic Spin Ordering on the (111) - (2 x 1) Surface of Diamond. Solid State Commun. 63, 335-339.

Ritsko JJ. (1979). Electron energy loss spectroscopy of pristine and radiation damaged polyethylene. J. Chem. Phys. 70, 5343-5349.

Rye RR, Madey TE, Houston JE, and Holloway PH. (1978). Chemical-state effects in Auger electron spectroscopy. J. Chem. Phys. 69, 1504-1512.

Rye RR, Houston JE, Jennison DR, Madey TE, and Holloway PH. (1979). Chemical information from Auger spectroscopy. Ind. Eng. Chem. Prod. Res. Dev. 18, 2-7.

Rye RR, Jennison DR, and Houston JE. (1980). Auger spectra of alkanes. J. Chem. Phys. 73, 4867-4874.

Rye RR, Greenlief CM, Goodman DW, Hardegree EL, and White JM. (1988). Auger spectra of C_2-hydrocarbons on Ni(100). Surf. Sci. 203, 101-124.

Rye RR. (1989). Correlation in the Auger Spectrum of Polyethylene. Phys. Rev. B 39, 10319-10324.

Sawatzky GA. (1977). Quasiatomic Auger spectra in narrow band metals. Phys. Rev. Letters 39, 504-507.

Seki K, Hashimoto S, Sato N, Harada Y, Ishii K, Inokuchi H, and Kanbe J. (1977). Vacuum ultraviolet photoelectron spectroscopy of hexatriacolane (n-$C_{36}H_{74}$) polycrystals: a model compound of polyethylene. J. Chem. Phys. 66, 3644-3649

Sickafus EN. (1971). A secondary emission analog for improved Auger spectroscopy with retarding potential analyzers. Rev. Sci Instr. 42,

933-941

Sickafus EN. (1977). Linearized secondary-electron cascades from the surfaces of metals I. Clean surfaces of homogeneous specimens. Phys. Rev. B116, 1436-1447.

Siegbahn K, (1969). ESCA Applied to Free Molecules (North Holland Publ. Co. New York), p. 103.

Weiss A, Mayer R, Jibaly M, Lei C, Mehl D, and Lynn KG. (1988). Auger-electron emission resulting from the annihilation of core electrons with low-energy positrons. Phys. Rev. Letter 61, 2245-2248.

Discussion with Reviewers

P.Schultz: I'd like to offer two comments regarding experimental techniques for studying Auger electron spectroscopy:
(i) A technique which is being pioneered by MacDonald (MacDonald JR, Feldman LC, Silverman PJ, Davies JA, Griffiths K, Jackman TE, Norton PR, and Unertl WN. (1983), Nucl. Instr. and Meth. in Phys. Res. 218 765-782.) is to use MeV ions. While the background is still a problem with this technique, it offers the capability of some surface and interface selectivity by taking advantage of channeling effects for both the incident beam and the emitted electrons.
(ii) Positron induced AES has fundamental differences from other techniques which should be remembered. A thermal positron trapped in the surface state is highly mobile, and most evidence suggests that all such positrons annihilate either from surface defects or impurities (Shultz, PJ and Lynn KG. (1988). Rev. Mod. Phys. 60, 701-785.) This means that Auger electrons emitted following positron-core electron annihilation are specifically sampled from surface irregularities, and not representative of average conditions (as is the case from energetic incident beams). This may be either an advantage or disadvantage, depending on the application.
Author: A disadvantage with normal ion induced Auger is that both solid and gas phase Auger spectra are often observed, in addition to the other satellites you mentioned. The gas phase spectra result from Auger decay of sputtered atoms, which can be kept to a minimum by use of the large ion energies you mentioned. I also agree with you that positron-induced AES can provide some very unique and interesting data.

MJ Dresser: How important are individual system properties on the shape of the backscattering, L(E), curve you describe? Could, for example, one hope to have a reasonable approximation for other systems using the curve you give at 140 eV, or must the backscattering experiment be done for each system and/or at each energy.
Author: L(E) is of course different for each material, since the loss spectrum reflects one electron and collective electron (plasmon) losses. L(E) can be conveniently measured at the same time as the Auger spectrum, so I recommend that it be obtained for each material, and measured at the energy of the principal Auger peak. However, we have found that it is very important that L(E) be measure in the N(E) mode, even if the Auger spectra was measured in the derivative mode, because the broad shape of L(E) is more critical to the deconvolution process, than the detailed structure in L(E). L(E) does not change strongly with energy above 100 eV, so that the primary beam energy is not that critical for the determination of L(E).

MJ Dresser: Are computer codes available to accomplish the deconvolution procedures required to arrive at A(E) from L(E) and A'(E). If so, in what language, where may they be found, and what sort of computer power is required?
Author: Yes, we have made both a fortran and basic versions of our codes available, along with a booklet of instructions for their use. These codes can be run on a PC computer, or on any main frame. I should mention, however, that background removal is not a simple, automatic procedure; control by an experienced observer is often necessary to assure proper convergence to the correct results.

RR Rye: One gets the feeling that your theoretical approach introduces a very large number of parameters for fitting the experimental spectra. To what extent are these independent, and to what extent can they be justified?
Author: As Table 1 indicates, we generally have 3 ΔU and 3 δ parameters available for the principal component, plus a multiplicative constant for the total intensity, since the experimental Auger intensity is arbitrary. However, often these parameters are set to zero. Thus for methane and diamond we had only one non-zero parameter, for graphite 2 parameters, and for polyethylene 3 parameters. These parameters are largely independent from each other; i.e. the ΔU parameters alter the shapes of the components and the δ parameters the energies. The satellites have additional parameters, which determine their relative intensities and their shapes and energies. We report only one or two significant figures for each parameter because of the level of uncertainties which exists. The systematic variation of these parameters from one material to the other suggests that these parameters are indeed justified and the values obtained are significant.

LW Hobbs: Recent work indicates that radiolylic damage in organic molecular crystals can originate from core electron excitations, presumably leading to Auger emission and hole-hole repulsions. Thus your suggestion of a Coulomb explosion blowing apart molecules is of considerable relevance. I cannot see, however, how this notion applies to ionic solids where the holes are localized on a single ion. Is it the response of the anomalous ion charge state to the prevailing Madelung potential that results in an unstable ion position?
Author: Indeed, this is the essence of the well-known Knotek-Feibelman theory for electron stimulated desorption (Knotek, 1978).

MJ Dresser: Presuming that an experimentalist had a "properly treated" set of AES data (i.e. A(E) by your prescription), from an unknown

carbon bearing species, can your procedure be inverted to determine the chemical nature of the carbon bonds represented in that Auger spectrum?
Author: Assuming a homogeneous material, one does not need to follow my prescribed procedure. The simple "finger prints" which I mentioned are sufficient to identify the nature of the carbon species (i.e. graphite, diamond, amorphous carbon etc). I think it would also be possible to distinguish between various hydrocarbons, directly from the "finger print". The motivation for developing my theoretical procedure is to obtain detailed bonding information, such as the extent of hybridization, electron delocalization, screening, and covalency existing in a material.

D Newbury: The materials scientists who are fabricating diamond or diamond-like films seem to often produce mixtures of different carbon allotropes on a very fine scale. Can you predict how well your Auger deconvolution/modelling technique would be able to separate components from a mixture of allotropes which occur in the same carbon Auger peak?
Author: These diamond-like carbon materials usually contain mixtures of graphitic, diamond-like, and amorphous carbon bonding. The differences in the Auger lineshapes for these different allotropic forms are more distinct in the dN(E)/dE form, so that again, it would probably be better to determine the components by utilizing the dN(E)/dE "finger prints".

K Krishnan: The optical properties of diamond-like carbon films are substantially modified by the addition of hydrogen in the magnetron sputtering process. Would it be possible to say something about the bonding of hydrogen in these films from Auger spectroscopy.
Author: Auger spectroscopy samples a localized density of states; i.e. local to the atom with the core hole. In general AES cannot distinguish between carbon-carbon and carbon-hydrogen bonds.

P Kruit: How distinct are the "finger prints" in AES compared with that in UPS?
Author: That depends on the materials compared. For the carbon materials (e.g. graphite, diamond, and the carbides), I think the "finger prints" are more distinct in AES, because these systems have widely different ΔU's. Within the alkane series, valence band UPS is much more distinctive, because the ΔU's in the Auger lineshapes are similar for all of the higher alkanes. Generally the "finger prints" in UPS are probably more distinctive than those in AES, unless one is comparing systems with widely different ΔU's. On the other hand, the chemical shifts in AES are generally equal to or larger than XPS core-level shifts.